



Quantized circulation in dilute Bose–Einstein condensates

T.P. Simula *, S.M.M. Virtanen, M.M. Salomaa

*Materials Physics Laboratory, Helsinki University of Technology P.O. Box 2200 (Technical Physics),
FIN-02015 HUT, Finland*

Abstract

We compute using a microscopic mean-field theory the structure and the quasiparticle excitation spectrum of a dilute, trapped Bose–Einstein condensate penetrated by an axisymmetric vortex line. The Gross–Pitaevskii equation for the condensate and the coupled Hartree–Fock–Bogoliubov–Popov equations describing the elementary excitations are solved self-consistently using finite-difference methods. We find locally stable vortex configurations at all temperatures below T_c . © 2001 Elsevier Science B.V. All rights reserved.

PACS: 02.70.Bf; 03.75.Fi; 67.40.Db

Keywords: Bose–Einstein condensation; Vortices; Finite-difference methods

1. Introduction

The long anticipated Bose–Einstein condensation in dilute, weakly interacting atomic gases was finally accomplished in 1995 [1–4]. Recently, the creation of quantized vortices in harmonically trapped Bose–Einstein condensates (BECs) was reported [5,6]. The commonly employed Gross–Pitaevskii (GP) equation has been successful in describing properties of BECs. However, it neglects the noncondensed gas component always present in such systems due to the interactions. Using the Hartree–Fock–Bogoliubov (HFB) quasiparticle formalism [7], this limitation of the GP approach is surpassed with the cost of computing the excitation spectrum of the system in a mean-field approximation. This, in turn, involves finding a large number of eigensolutions to a system of coupled partial

differential equations. The computational challenge is further aggravated by the self-consistency requirement implying use of iteration in solving the equations.

Altogether, there exists a number of approximative theoretical methods for studying the properties of inhomogeneous BECs [8]. The mean-field description was originally due to Bogoliubov [9]. It has been used widely, starting in 1996 by Burnett and co-workers, to numerically study trapped condensates [10,11]. The self-consistent Popov version of the HFB formalism has also been used to investigate the microscopic structure of quantized vortices in BECs [12,13].

In this paper, we describe the computational techniques used by us in finding self-consistent solutions to the coupled HFB–Popov and GP equations describing dilute Bose–Einstein condensates. In Section 2, we present the mean-field equations for a harmonically trapped condensate with an axial vortex line. Section 3 focuses on the computational aspects involved.

* Corresponding author.

E-mail address: Tapio.Simula@hut.fi (T.P. Simula).

2. Cylindrical condensate and an axisymmetric vortex line

We consider a harmonically trapped, dilute and weakly interacting BEC with a quantized, axially symmetric vortex line located along the z -axis of a cylindrical coordinate system $\mathbf{r} = (r, \theta, z)$. The trapping potential is assumed to have the form $V_{\text{tr}}(\mathbf{r}) = \frac{1}{2}M\omega^2 r^2$, where M is the atom mass and ω is the radial trapping frequency. The vortex line is described through the complex phase factor of the condensate wavefunction $\phi(\mathbf{r}) = \phi(r)e^{im\theta}$, where the integer m denotes the number of circulation quanta in the vortex. Here we restrict to singly quantized vortices with $m = 1$. The formalism we present is the Popov approximation to the Hartree–Fock–Bogoliubov mean-field theory [7].

The condensate wavefunction $\phi(\mathbf{r})$ and the chemical potential μ satisfy the generalized GP equation [7]

$$[\mathcal{H}_0(\mathbf{r}) + g|\phi(\mathbf{r})|^2 + 2g\rho(\mathbf{r})]\phi(\mathbf{r}) = \mu\phi(\mathbf{r}), \quad (1)$$

where $\rho(\mathbf{r})$ is the particle density of the noncondensed gas, the single particle Hamiltonian $\mathcal{H}_0(\mathbf{r}) = -\hbar^2\nabla^2/2M + V_{\text{tr}}(\mathbf{r})$, and g is the interaction coupling constant.

The quasiparticle amplitudes $u_q(\mathbf{r})$, $v_q(\mathbf{r})$ and the excitation eigenenergies E_q are obtained from the coupled differential equations [7]

$$\begin{aligned} \mathcal{L}(\mathbf{r})u_q(\mathbf{r}) + g\phi^2(\mathbf{r})v_q(\mathbf{r}) &= E_q u_q(\mathbf{r}), \\ \mathcal{L}(\mathbf{r})v_q(\mathbf{r}) + g\phi^{*2}(\mathbf{r})u_q(\mathbf{r}) &= -E_q v_q(\mathbf{r}), \end{aligned} \quad (2)$$

where $\mathcal{L}(\mathbf{r}) \equiv \mathcal{H}_0 - \mu + 2g|\phi(\mathbf{r})|^2 + 2g\rho(\mathbf{r})$. The eigensolutions of Eqs. (2) self-consistently determine the noncondensate density $\rho(\mathbf{r})$ via the equation

$$\rho(\mathbf{r}) = \sum_q [(|u_q(\mathbf{r})|^2 + |v_q(\mathbf{r})|^2) n(E_q) + |v_q(\mathbf{r})|^2]. \quad (3)$$

Above, q labels the set of radial, angular, and axial quantum numbers (q_r, q_θ, q_z) and $n(E_q) = (e^{E_q/k_B T} - 1)^{-1}$ is the Bose–Einstein distribution function containing explicitly the temperature dependence of the system. It is worth noting the symmetry property of the solutions to the HFB–Popov equations: $(u_q, v_q, E_q, q_\theta) \leftrightarrow (v_q, u_q, -E_q, -q_\theta)$, which may be used to slightly reduce the computational effort.

3. Numerical techniques

The nonlinear GP equation requires a numerical solution for inhomogeneous systems. A very large number of eigensolutions has to be computed in order to calculate the sum in Eq. (3) with sufficient accuracy. Furthermore, the requirement of self-consistency increases the computational challenge.

The procedure for solving Eqs. (1)–(3) is summarized below:

- obtain $\phi(\mathbf{r})$ and μ from the Eq. (1),
- calculate the eigensolutions u_q , v_q , and E_q from Eqs. (2),
- compute the noncondensate density $\rho(\mathbf{r})$ from Eq. (3),
- iterate the process until $\phi(\mathbf{r})$ and $\rho(\mathbf{r})$ have converged to predefined accuracies.

Due to the cylindrical symmetry, the quasiparticle amplitudes can be separated to radial, angular and axial factors and, consequently, Eqs. (1)–(3) reduce to solving computationally only the corresponding radial equations. Dirichlet boundary conditions are set on the boundaries of the computational region. The condensate wavefunction vanishes also on the vortex axis due to requirement of continuity. Periodic boundary conditions are imposed in the axial direction, thus modeling a system in the limit of a very weak axial trapping potential.

The noncondensate density $\rho(\mathbf{r})$ and the condensate wavefunction $\phi(\mathbf{r})$ are first initialized, either using an educated guess or data obtained from previous computations. After an appropriate scaling of variables, the GP equation for a fixed value of μ is solved on an evenly distributed real-space lattice, employing a relaxation method. A central finite-difference discretization formula is applied to approximate the derivative operator. In order to accelerate the convergence, we use overrelaxation by choosing

$$\phi_i^{\text{new}}(\mathbf{r}) = s\phi_i(\mathbf{r}) + (1-s)\phi_{i-1}(\mathbf{r}), \quad (4)$$

where i labels the iteration cycle and $s > 1$ ($s < 1$) is the over(under)relaxation parameter. After the condensate wavefunction $\phi(\mathbf{r})$ has converged to the solution, see Fig. 1, the total particle number $N = \int [|\phi(\mathbf{r})|^2 + \rho(\mathbf{r})] d\mathbf{r}$ is computed. The chemical potential is then increased or diminished accordingly, and $\phi(\mathbf{r})$ is recomputed. The procedure is repeated until μ is consistent with the fixed particle number.

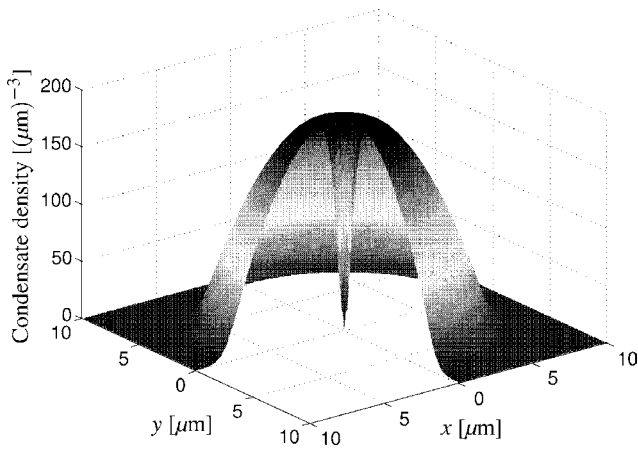


Fig. 1. Computed radial density distribution of the condensate particles for a singly quantized vortex configuration at $T = 50$ nK. Particles are radially confined by a harmonic trapping potential. The condensate circulates around the cylinder axis and vanishes in the vortex core. The computations are performed with the same physical parameters as in Refs. [12,13].

Most of the CPU time is consumed in the computation of the matrix eigensolutions of the HFB–Popov equations. We use high-order finite-difference discretization, combined with a fast band-matrix solver to compute the quasiparticle eigenstates. The discretization yields a nonsymmetric matrix with bandwidth $2j - 1$, where j is the order of the finite-difference formula used. We solve the matrix eigenvalue problem using the ARPACK software [14] which implements an implicitly restarted Arnoldi method.

In order to compute $\rho(\mathbf{r})$ with high accuracy, see Eq. (3), also the contributions of high-energy quasiparticle states have to be included. We take into account the contributions of states with $E_q > 45\hbar\omega$ by using for them a local-density approximation (LDA) [15]. In the LDA, the system is treated locally as if it were homogeneous. At low temperatures ($T \lesssim T_c/10$), the contribution of the LDA to $\rho(\mathbf{r})$ becomes negligible, but for increasing temperature, the dominant contribution to the noncondensate density is given by the LDA. Fig. 2 shows the temperature dependence of the total particle number as a function of the radial distance from the vortex axis.

All equations are treated on an evenly spaced grid. Typically, we use an eleven-point finite-difference formula to discretize the HFB–Popov equations. This is found to be rather optimal in view of accuracy and computing time, which grows with increasing

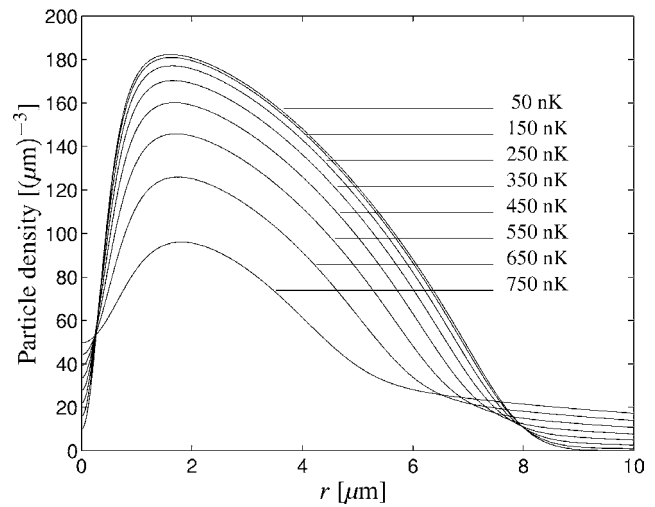


Fig. 2. Temperature dependence of the total particle density as a function of radial distance from the vortex axis. Below the Bose–Einstein condensation temperature $T_c \approx 1$ μ K, the number of particles in the condensate increases rapidly with decreasing temperature. Note the finite noncondensate density on the vortex axis. It is precisely this finite quantum depletion out of the condensate which renders the vortex locally stable even in the $T = 0$ limit.

bandwidth of the discretization matrix. Depending on the system, we need to calculate some 50 lowest eigensolutions for each (q_θ, q_z) -combination. In total, this amounts to 10^4 – 10^5 eigenvalues to be computed. However, since the execution time for ARPACK grows rapidly with the number of requested eigensolutions, we only compute some 20 of them at a time. The relative accuracy in E_q is 10^{-4} – 10^{-7} , the high-lying states being the most precise. Part of the computed quasiparticle excitation spectrum is displayed in Fig. 3.

To obtain smooth convergence, we employ under-relaxation, see Eq. (4), in updating $\rho(\mathbf{r})$ between the iteration cycles. As the lowest quasiparticle energy E_0 tends to zero for decreasing temperature, the value of the sum in Eq. (3) becomes highly sensitive to changes in E_0 , due to the large derivative of the Bose factor at E_0 . Consequently, the iteration may diverge unless the equilibrium value is approached ‘adiabatically’. Generally it takes 5–20 iterations to find a self-consistent solution for a given temperature. The criterion for terminating the iteration is that the maximum relative change in $\rho(\mathbf{r})$ and $\phi(\mathbf{r})$ are smaller than predefined error tolerances.

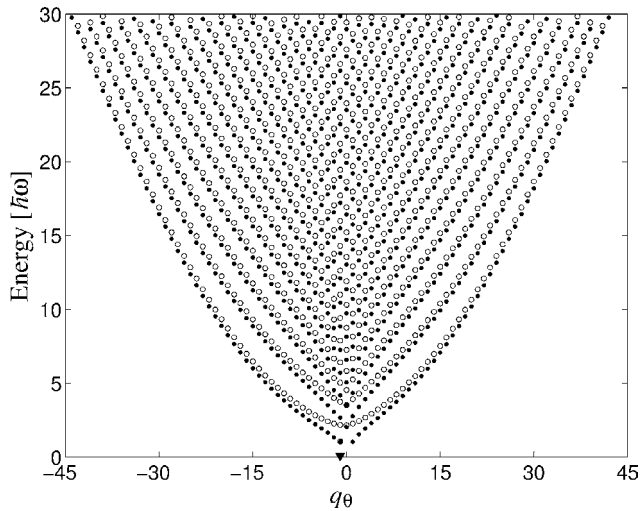


Fig. 3. Part of the quasiparticle excitation spectrum for $q_z = 0$ (●) and $q_z = 1$ (○) as a function of the angular-momentum quantum number, q_θ . The lowest collective mode (▼) is positive, which implies the vortex to be locally energetically stable. This particular state makes the iteration a delicate process due to the sensitive Bose factor, $n(E_0)$, at low temperatures. The lowest mode is intimately related to the vortex precession around the vortex axis found in the experiments [17,18].

The justification for the methods described above has been verified using various validity checks. The ground-state solution for $\phi(\mathbf{r})$ can be explicitly checked to satisfy the GP equation with subsequent numerical differentiation; the condensate wavefunction $\phi(\mathbf{r})$ is also obtained from the HFB–Popov equations with $E_q = 0$. Furthermore, independent solutions of both the HFB–Popov and GP equations have been computed using shooting methods. The correct convergence of $\phi(\mathbf{r})$ and $\rho(\mathbf{r})$ is inspected both visually and using different initializations and convergence criteria.

4. Discussion

In conclusion, we have computed the structure and the excitation spectrum for a vortex line in a dilute atomic Bose–Einstein condensate using a self-consistent microscopic theory. An efficient numerical scheme is employed. Further advance could be obtained by applying the parallel version of ARPACK software. We find locally energetically stable configurations for all temperatures below T_c , implying that the vortex state is (meta)stable within the self-consistent

theory used [13]. This result demonstrates the self-stabilizing mechanism of the noncondensed gas always present in an interacting system. However, this effect only appears within the self-consistent theories. If the noncondensate is neglected as in the Bogoliubov approximation, negative quasiparticle excitation energies emerge, implying local energetic instability of the vortex state [16]. The fact that the recent experiments [17] support the prediction of the nonself-consistent theories could be due to an insufficient thermalization in the vortex core. To improve comparison with experiments, a fully 3D computation would have to be performed. The method could also be applied, e.g., to multi-component spinor condensates.

Acknowledgements

We thank the Center for Scientific Computing (CSC, Finland) for computer resources. This work has been supported by the Academy of Finland through the Grant “Theoretical Materials Physics”, the Graduate School in Technical Physics, and by the Alfred Kordelin Foundation (travel grant to TPS).

References

- [1] F. Dalfovo, S. Giorgini, L.P. Pitaevskii, S. Stringari, *Rev. Mod. Phys.* 71 (1999) 463.
- [2] M.H. Anderson, J.R. Ensher, M.R. Matthews, C.E. Wieman, E.A. Cornell, *Science* 269 (1995) 198.
- [3] C.C. Bradley, C.A. Sackett, J.J. Tollett, R.G. Hulet, *Phys. Rev. Lett.* 75 (1995) 1687.
- [4] K.B. Davis, M.-O. Mewes, M.R. Andrews, N.J. van Druten, D.S. Durfee, D.M. Kurn, W. Ketterle, *Phys. Rev. Lett.* 75 (1995) 3969.
- [5] M.R. Matthews, B.P. Anderson, P.C. Haljan, D.S. Hall, C.E. Wieman, E.A. Cornell, *Phys. Rev. Lett.* 83 (1999) 2498.
- [6] K.W. Madison, F. Chevy, W. Wohlleben, J. Dalibard, *Phys. Rev. Lett.* 84 (2000) 806.
- [7] A. Griffin, *Phys. Rev. B* 53 (1996) 9341; D.A.W. Hutchinson, R.J. Dodd, K. Burnett, *Phys. Rev. Lett.* 81 (1998) 2198; N.P. Proukakis, S.A. Morgan, S. Choi, K. Burnett, *Phys. Rev. A* 58 (1998) 2435.
- [8] K. Huang, P. Tommasini, *J. Res. Natl. Inst. Stand. Technol.* 101 (1996) 435.
- [9] N. Bogoliubov, *J. Phys. (Moscow)* 11 (1947) 23.
- [10] M. Edwards, P.A. Ruprecht, K. Burnett, R.J. Dodd, C.W. Clark, *Phys. Rev. Lett.* 77 (1996) 1671.
- [11] D.A.W. Hutchinson, E. Zaremba, A. Griffin, *Phys. Rev. Lett.* 78 (1997) 1842.

- [12] T. Isoshima, K. Machida, *Phys. Rev. A* 59 (1999) 2203.
- [13] S.M.M. Virtanen, T.P. Simula, M.M. Salomaa, *Phys. Rev. Lett.* 86 (2001) 2704.
- [14] Software available from the ARPACK Home Page at Comp. and Appl. Math. Dept., Rice Univ., <http://www.caam.rice.edu/software/ARPACK/>.
- [15] J. Reidl, A. Csordás, R. Graham, P. Szépfalussy, *Phys. Rev. A* 59 (1999) 3816.
- [16] D.S. Rokhsar, *Phys. Rev. Lett.* 79 (1997) 2164.
- [17] B.P. Anderson, P.C. Haljan, C.E. Wieman, E.A. Cornell, *Phys. Rev. Lett.* 85 (2000) 2857.
- [18] A.A. Svidzinsky, A.L. Fetter, *Phys. Rev. Lett.* 84 (2000) 5919.